NASA Technical Memorandum 4158
DOT/FAA/DS-89/35

Relative Merits of Reactive and Forward-Look Detection for Wind-Shear Encounters During Landing Approach for Various Microburst Escape Strategies

David A. Hinton

FEBRUARY 1990

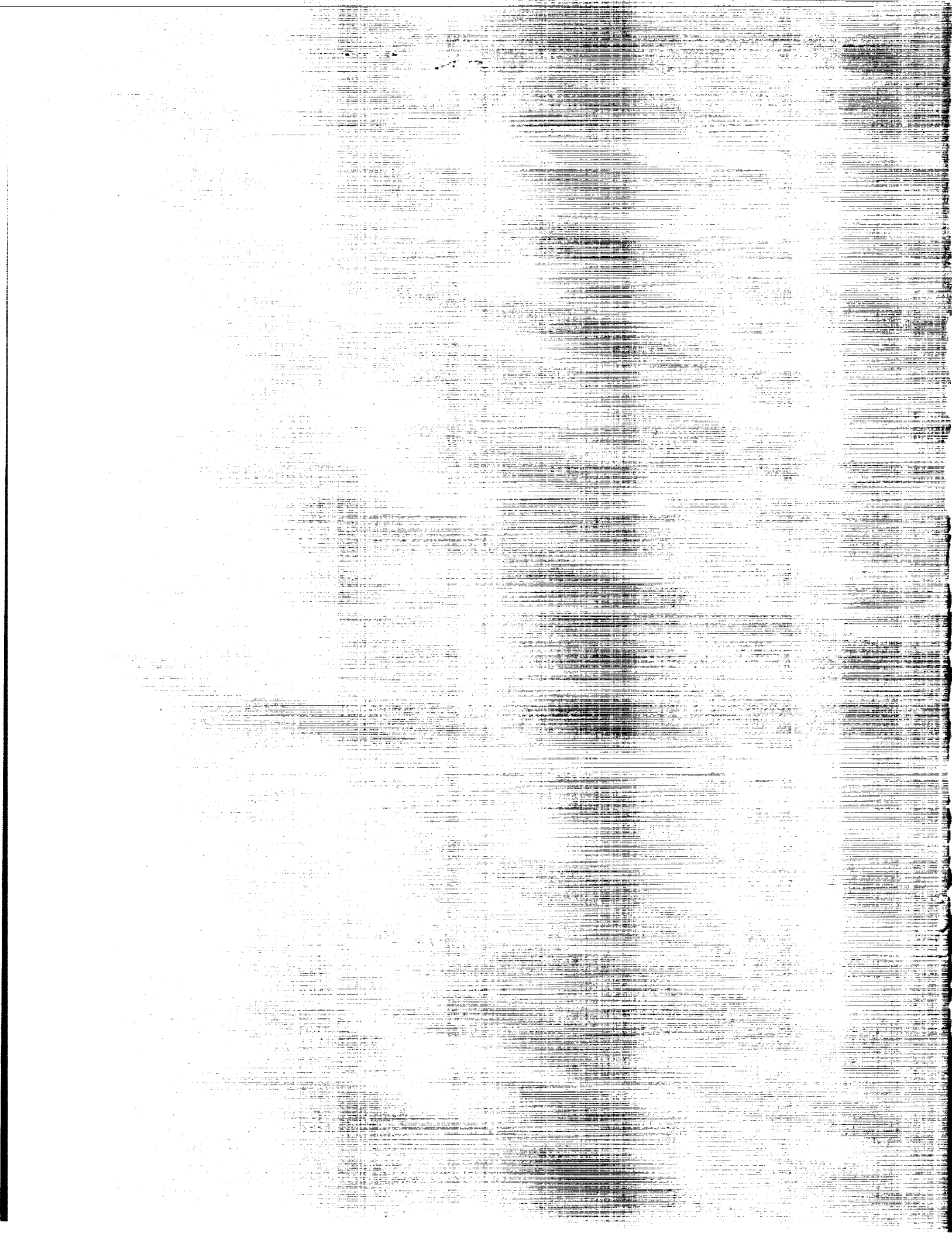

NASA Technical Memorandum 4158
DOT/FAA/DS-89/35

Relative Merits of Reactive and Forward-Look Detection for Wind-Shear Encounters During Landing Approach for Various Microburst Escape Strategies

David A. Hinton
Langley Research Center
Hampton, Virginia

National Aeronautics and
Space Administration
Office of Management
Scientific and Technical
Information Division

1990

Summary

An effort is in progress by the National Aeronautics and Space Administration (NASA), the Federal Aviation Administration (FAA), and industry to reduce the threat of convective microburst windshear phenomena to aircraft through hazard characterization, improved wind-shear detection and warning, development of recovery flight techniques, and crew training. The goals of this study were to quantify the benefits of forward-look sensing capabilities and to develop and test a candidate set of strategies for recovery from inadvertent microburst encounters during the landing approach, given the utilization of both reactive-only and forward-look wind-shear detection. The assumptions were made that the presence of the microburst could be detected but that the structure and strength of the flow field ahead of the airplane were not known. Candidate strategies were developed and evaluated using a nonpiloted simulation consisting of a simple point-mass performance model of a transport-category airplane flying through an analytical microburst model.

The results of this study indicate that the factor that most strongly affects a microburst recovery is the time at which the recovery is initiated. In nearly all microburst situations evaluated, quickening the alert and recovery initiation by 5 sec provided a greater increase in recovery performance than could be achieved by changing the recovery strategy. Forward-look alerts given 10 sec prior to microburst entry permitted recoveries to be made with negligible altitude loss. The results also show that no single microburst scenario can be used to evaluate the relative merits of various recovery strategies. If a strategy was chosen that performed best for the majority of the tested microburst scenarios, a scenario could be found for another strategy performed better. The type of alert used to initiate the recovery (reactive or forward-look) and the altitude of the microburst encounter had an effect on the type of recovery strategy that performed best. These factors may have serious implications for the design and certification of wind-shear systems. The baseline recovery strategy was an approximation of the manual wind-shear recovery technique that is currently being taught to air-carrier crews. This strategy compared favorably with the proposed advanced recovery strategies in the microburst scenarios that the manual technique was designed to accommodate.

Introduction

Numerous air-carrier accidents and incidents have resulted from inadvertent encounters with the atmospheric wind-shear associated with microburst phenomena; some of these accidents have resulted in heavy loss of life. A microburst is a strong, localized downdraft that strikes the ground, producing winds that diverge radially from the impact point. An airplane penetrating the center of a symmetric microburst initially encounters an increasing head wind, which improves airplane climb-angle performance, and then encounters a strong downdraft and a rapidly increasing tail wind. The effects of the downdraft and increasing tail wind may easily exceed the climb and acceleration capabilities of the airplane, which would cause an unavoidable loss of altitude and airspeed. These encounters have resulted from the fact that the microburst and its impact on airplane performance have been recognized for only a relatively short time (refs. 1 and 2), and from the fact that the ability to reliably predict or detect a microburst in an airplane's flight path, in an operational environment, does not yet exist. The physics of microburst winds have only recently been understood in detail, and recovery during inadvertent airplane encounters may require techniques that are unique to microbursts and counterintuitive to flight crews (ref. 3).

Previous research has been conducted on control strategies for maintaining a given flight path in the presence of strong wind shears (refs. 4 and 5). These studies have developed control laws to permit the airplane to track a predefined path, such as the glide slope of an instrument landing system. This tracking will be possible in many wind-shear encounters, but will not be possible if the shear is severe. With currently available sensors, the severity of a shear cannot be known until the airplane has successfully flown through it. Other research (refs. 6 and 7) has shown the performance available from an airplane following an optimal trajectory when full knowledge of the microburst flow field is available prior to the encounter. In those studies, the emphasis was on escape from inadvertent microburst encounters, and the trajectory was a result of the optimization procedure, not an assumed goal. Other research by the same authors considered wind-shear recovery performance when only local wind knowledge is available (refs. 8 and 9). The application of these optimal recovery concepts to practical recovery-strategy development was studied (ref. 10), and the performance of those recovery strategies in piloted operations, in the takeoff encounter case, was evaluated in the simulator study described in reference 3. The studies described in references 3 and 10 showed that advanced recovery strategies enabled recovery to take place at higher minimum altitudes than with constant pitch techniques, but that recovery altitude was very sensitive to small deviations in airplane pitch history. The best

recovery techniques, from a performance perspective, were counterintuitive to the pilots. The counterintuitive nature of the recoveries and the sensitivity of the recovery performance combined to produce experimental variations in performance between piloted runs that were greater than the differences in performance between the various strategies tested. Thus, the predicted advantages of the advanced strategies were not always realized in piloted operations.

Following the NASA efforts in takeoff recovery strategies, an effort was initiated to develop recovery concepts for the more complex approach-to-landing encounter case. This case is more complex because of the additional variables of engine thrust and possible configuration changes. Advances in forward-look, wind-shear sensor technologies have also raised the issues of how much forward-look distance is necessary for airplane survival and how recovery concepts will be affected by forward-look data. These questions were studied as a part of the investigation of this report.

An effort aimed at quantifying the benefits of forward-look sensing and developing recovery-strategy concepts for the approach-to-landing case wind-shear encounter, given the utilization of both reactive-only and forward-look wind-shear detection, is described in this paper. Reactive detection and alerting is derived from aircraft inertial and air data sensors, and forward-look detection and alerting is derived from remote measurements of wind fields that the aircraft has not yet encountered. This effort was performed in preparation for a future piloted simulation study and utilized analytical analysis of airplane performance in wind-shear and nonpiloted simulations of wind-shear encounters. The nonpiloted simulation consisted of a point-mass performance model of a transport-category airplane flying through an analytical microburst model. It was assumed that the wind field ahead of the airplane was not known in sufficient detail for use in recovery algorithms; the forward-look detection could only provide a discrete alert that a wind shear existed ahead of the airplane. Lessons learned from previous and ongoing research were used to develop six candidate microburst escape strategies. The characteristics of these strategies were then evaluated and compared with the current industry-approved manual recovery technique (ref. 11). The sensitivity of the candidate recovery strategies to variations in microburst location and to the timing of the wind-shear detection was examined.

Symbols

Values are expressed in U.S. Customary Units. A dot above the symbol denotes a derivative with respect to time. The units presented were used in derivations and computer software. Units in common use in the aircraft industry were used in cockpit displays and for discussion in the text; these units are shown below in parentheses.

D	airplane total drag, lbf
E	airplane total energy, ft-lbf
E_s	specific total energy (energy per unit weight), also called energy height, ft
ΔE_s	change in energy height, ft
E_u	useful specific total energy, energy height in excess of energy height at $1g$ stick-shaker airspeed, ft
F	"F-factor" measure of wind-shear impact on capability of airplane flight-path angle, rad
FAA	Federal Aviation Administration
g	gravitational acceleration ($1g$ = 32.2 ft/sec^2)
H_{gs}	altitude of glideslope at airplane position, ft
H_o	initial airplane altitude for a run, ft
H_{ref}	reference altitude in control laws, ft
h	airplane altitude, ft
h_p	potential altitude, ft
K	gain in flight-path-angle control law
L	airplane total lift, lbf
m	airplane mass, slugs
T	total engine thrust, lbf
Δt	time-step size in nonpiloted simulation program, sec
V	airplane true airspeed, ft/sec (knots)
V_i	airplane inertial velocity, ft/sec (knots)
V_{ref}	reference airspeed for landing approach, knots
V_{ss}	airspeed at which stick shaker activates in $1g$ flight, knots

W	airplane weight, lbf
W_h	vertical wind speed, up positive, ft/*sec* (ft/min)
W_x	horizontal wind speed, tail wind positive, ft/sec (knots)

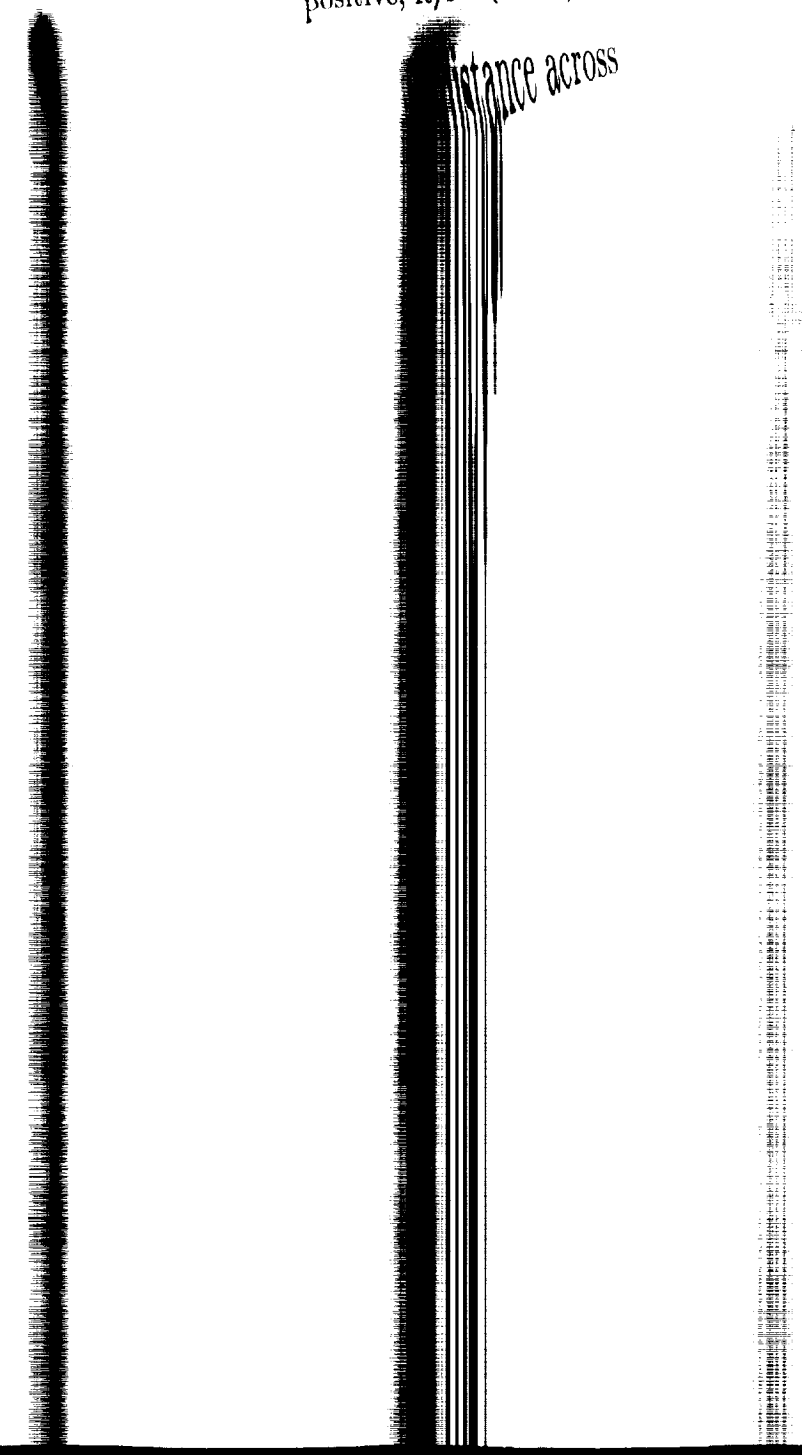

altitude above the ground that is relevant to the recovery. Airplane total energy is then defined as

$$E = 0.5mV^2 + mgh \tag{1}$$

where V is airspeed, m is airplane mass, g is gravitational acceleration, and h is altitude. The specific total energy (E per unit weight), or energy height, is defined as

V^2 (2)

W	airplane weight, lbf
W_h	vertical wind speed, up positive, ft/sec (ft/min)
W_x	horizontal wind speed, tail wind positive, ft/sec (knots)
x	horizontal distance across ground, ft
α	wing angle of attack, rad (deg)
α_{ss}	angle of attack that activates stick shaker, rad
γ_a	air-mass flight-path angle, rad
γ_c	commanded inertial flight-path angle, rad
γ_i	inertial flight-path angle, rad
$\gamma_{i,p}$	inertial potential flight-path angle, rad
γ_{limit}	minimum γ_c allowed, prevents descent below glide slope, rad
θ	airplane pitch attitude, rad
θ_{err}	pitch-attitude error, rad
θ_s	target pitch attitude in wind shear, rad
λ	gain in acceleration strategy

Airplane Energy-Height Concepts

In an effort to determine the amount of forward-look detection necessary for airplane survival, an analysis of airplane energy height during a microburst encounter was performed. The purpose of the analysis was to gain insight into the effects of microburst strength and detection delays (reactive systems) or advances (forward-look systems) on airplane survivability by examining the changes in energy height during an event. The concepts of airplane total energy and potential flight-path angle were discussed in reference 10, and equations are repeated herein as necessary. The airplane flight path and the wind components are related by the coordinate system shown in figure 1.

The airplane total energy is defined as the sum of the air-mass relative kinetic energy and the inertial potential energy. Air-mass kinetic energy is used since only airspeed, not ground speed, describes the ability of the airplane to climb or maintain altitude. Inertial potential energy is likewise used since it is altitude above the ground that is relevant to the recovery. Airplane total energy is then defined as

$$E = 0.5mV^2 + mgh \tag{1}$$

where V is airspeed, m is airplane mass, g is gravitational acceleration, and h is altitude. The specific total energy (E per unit weight), or energy height, is defined as

$$E_s = \frac{V^2}{2g} + h \tag{2}$$

The rate of change of E_s is also the potential rate of climb of the airplane, assuming a negligible energy loss when trading airspeed for climb rate, and is defined as

$$\dot{E}_s = \dot{h}_p = V\left(\frac{\dot{V}}{g}\right) + \dot{h} \tag{3}$$

By subtracting the energy-height component corresponding to the airplane stick-shaker airspeed V_{ss} from energy height, the useful energy height can be obtained as follows:

$$E_u = \frac{V^2}{2g} - \frac{(V_{ss})^2}{2g} + h \tag{4}$$

At the stick-shaker airspeed, airplane altitude is the same as the useful energy height. From reference 10, the inertial flight-path angle can be determined as follows:

$$\gamma_i = \frac{T - D}{W} - \frac{\dot{W}_x}{g} + \frac{W_h}{V} - \frac{\dot{V}}{g} \tag{5}$$

where T is airplane thrust, D is airplane drag, and W is airplane weight. The two wind terms describe the wind-shear impact on the climb-angle capability of the airplane, in terms of the horizontal shear $\dot{W}_x$ and vertical wind speed W_h, and are referred to as the "F-factor" (ref. 10), where

$$F = \frac{\dot{W}_x}{g} - \frac{W_h}{V} \tag{6}$$

By setting the airspeed rate to zero in equation (5), the potential inertial flight-path angle is obtained. Multiplying the potential inertial flight-path angle by airspeed produces a small angle approximation to the potential rate of climb as follows:

$$\gamma_{i,p} = \frac{T - D}{W} - F \tag{7}$$

$$\dot{h}_p = V\left(\frac{T - D}{W} - F\right) \tag{8}$$

Since the potential rate of climb is also the rate of change of energy height, equation (8) can be integrated during a wind-shear event to determine the change in energy height. Figure 2 shows the scenario used in the energy-height analysis. The width of the wind shear was fixed at 5000 ft. An event is defined as beginning upon receiving a wind-shear alert, in the case of forward-look detection, or upon entering the wind shear, in the case of a reactive alert. In both cases, the event end is defined as the point where the airplane exits the wind shear. For simplicity in conducting the analysis, the following assumptions were made:

1. While in the wind shear, the F-factor is constant; outside the wind shear, the F-factor is zero.
2. Only two values, the approach value and a go-around value, are used for the quantity $(T - D)/W$.
3. Approach airspeed is constant before reaching the shear, but, in the shear, the average of the approach speed and the stick-shaker speed is used in the calculations.

These assumptions permitted a very simple program to be constructed that provided insight into wind-shear recoveries. The effects of different airplane trajectories through the shear or different pitch time histories are not considered in the energy-height analysis; therefore, no attempt is made to predict the actual altitude of an airplane during an encounter. However, by comparing the change in energy height during an event with the useful energy height at the beginning of the event, an estimate of the best performance available from the airplane in that particular shear is obtained.

In the results to be presented, data for a Boeing 737-100 airplane were used. The configuration had the landing gear down, flaps were set at 25°, the gross weight was 90 000 lb. In this configuration, the reference approach speed was 137 knots, and the stick-shaker speed at go-around thrust was estimated to be 107 knots. The value of $(T - D)/W$ was -0.05 on the approach and was estimated to be 0.16 at go-around thrust. The change in energy height was calculated for various values of the F-factor and for various values of alert time, ranging from 20 sec after the encounter (-20 sec) to 60 sec before the encounter. A negative alert time indicates an alert received after entering the shear, which simulates a reactive system or pilot recognition of the shear; a positive alert time indicates an alert received prior to shear entry, which simulates a forward-look device.

Nonpiloted Simulation Models

The nonpiloted simulation consisted of a point-mass airplane model, an analytical microburst model, and a simple wind-shear detection scheme.

Airplane Model

The airplane model was based on a Boeing 737-100 flying in a vertical plane. No roll or yaw freedom was allowed. The gross weight was set at 90 000 lb, and sea-level standard atmospheric conditions were assumed. The airplane model was an enhancement of the model described in reference 10. The enhancements included (1) variable flap settings during a run, from 1° to 30°; (2) variable landing-gear positions; (3) an autothrottle for the approach phase; and (4) trim routines that initialized thrust and pitch attitude, in the presence of wind and at a given airspeed, for runs begun on an instrument landing system (ILS) glide slope.

Three configurations were used to set target flap, gear, and thrust settings. In configuration A, used for approach, the wing flaps were set to 25°, the gear was down, and the thrust was initialized at a trim value before the run and controlled by an autothrottle during the run. In configuration B, used for a go-around, the wing flaps were retracted to 15°, the gear was raised, and the thrust was set to 24 000 lb (maximum-rated thrust). In configuration C, used for escape maneuvers, the wing flaps and landing gear were left in the position called for by the last active mode, and the thrust was set to 24 000 lb. This latter configuration emulates the training-aid procedure (ref. 11), which calls for a constant airplane configuration to be maintained and for maximum-rated thrust to be used during a recovery. The rate of change of thrust was limited to 6000 lb/sec, and the flap rate was limited to 3.9° per second. Changes in landing-gear position were instantaneous.

Microburst Model

The microburst model (ref. 12) represents an axisymmetric stagnation-point flow that satisfies mass continuity and includes boundary-layer effects near the ground. The boundary-layer effects and spatial variation in outflow and downflow closely match real-world observations. The model permits a particular microburst to be simulated by specifying the following three characteristic parameters: (1) radius of downflow, (2) maximum outflow wind speed, and (3) the altitude at which the maximum outflow occurs. The maximum outflow occurs at a radius 12 percent greater than the radius of downflow. For this effort, the analytical model was fitted to microburst data generated by the Terminal-Area Simulation System (TASS) numerical microburst program (refs. 13 and 14), where the input condition to the program was an atmospheric sounding taken at Denver, Colorado on June 30, 1982. The resulting microburst has a maximum outflow of 37 knots

at an altitude of 120 ft and at a radius of 2391 ft. The radius of downflow is 2133 ft. Figure 3 shows the outflow and downdraft speeds as functions of altitude. The outflow is shown at the maximum outflow radius, and the downdraft is shown at the core. Figure 4 shows the outflow and downdraft speeds as functions of distance from the microburst core. The wind speeds are plotted for altitudes of 120 ft and 500 ft. The figures show the boundary-layer effect on the horizontal wind and show the reduction in outflow and increase in downdraft as altitude is increased above 120 ft. Although the plots resemble previous sine-wave approximations to a microburst, exponential functions are used to more closely approximate real-world observations of the gradual head-wind increase entering the shear and the much steeper wind gradient while in the shear.

Wind-Shear Detection

Wind-shear detection logic was used to activate the recovery control laws. The detection was based on the F-factor of the wind shear. An F-factor threshold of 0.15 was used to determine when the shear had been entered. An F-factor value of 0.05 was then used to determine when the shear had been exited. The measured F-factor values were not only dependent on spatial location in the microburst model, but also on airplane altitude, flight path, and airspeed. Variable time advance and delay were implemented to simulate forward-look sensors and reactive device delays. The advance is defined as the number of seconds that the alert is given in advance of the time that the threshold F-factor would have been exceeded if no alert had been given. The delay is defined as the number of seconds that the alert is given after the time that the threshold F-factor is exceeded. A delay of 5 sec is considered to approximate the response of realizable reactive detection systems. The recovery control laws use the two detection discrete signals (triggered by F-factor) to begin the recovery strategy, to determine control-law gains that are dependent on the alert type, and to transition to a normal climb-out after exiting the shear.

Candidate Wind-Shear Recovery Strategies

Each of the recovery control laws controlled the airplane model by calculating the pitch attitude needed to satisfy the strategy objectives. This target pitch attitude was compared with the actual pitch attitude, and a pitch rate was generated to null the difference. The control law for each strategy limited the target pitch attitude to the value that would place the airplane at the stick-shaker angle of attack. Also, the pitch rate was limited to 0.05 rad (3°) per second.

In each experimental run, the airplane was initialized on a glide slope at an approach speed of 137 knots. The glide slope was tracked and the autothrottle attempted to maintain airspeed. Upon activation of the wind-shear discrete, the recovery control law was activated. In each recovery, the thrust was increased to the maximum rated value of 24 000 lb and, except for the normal go-around recovery procedures, the landing-gear and wing-flap positions were held constant. Upon exiting the wind shear, a flight-path angle of 0.13 rad (7.4°) was targeted.

The baseline recovery strategy was the manual recovery technique currently in use by the industry. The other strategies were named (1) pitch, (2) acceleration, (3) flight-path angle, (4) level, (5) glide slope, and (6) go-around strategies. These strategies are described in this section. The control laws for implementing each of the recovery strategies are shown in figure 5. Most of the strategies have a parameter or gain that can be varied. The gains used to generate the data for this report were determined during a parametric study to provide the best recovery performance for each strategy; these gains are summarized in table 1.

Manual strategy. Since this strategy was designed to be flown manually in the absence of guidance commands (ref. 11), the exact procedure used will vary slightly from pilot to pilot. For this effort, the manual recovery was approximated by rotating the airplane to a pitch attitude of 0.26 rad (15°). This pitch attitude was maintained if it produced a zero or positive flight-path angle. If 15° of pitch was insufficient to maintain level flight, however, the control law would further increase pitch in an attempt to maintain level flight.

Pitch strategy. This strategy was a simplification of the manual recovery technique, in that a constant pitch attitude was maintained during the recovery regardless of the airplane flight-path angle. This strategy has been used as a baseline strategy in previous recovery studies (ref. 10). A pitch attitude of 0.23 rad (13°) was used.

Acceleration strategy. The acceleration strategy was an attempt to distribute excess airspeed (i.e., the airspeed margin above the $1g$ stick-shaker speed) across the wind-shear event. This goal was accomplished by reducing airspeed at a rate determined by the instantaneous F-factor of the wind shear. The

governing equation of the acceleration control law is

$$\frac{\dot{V}}{g} + \lambda F = 0 \tag{9}$$

where λ is a gain. A gain of 0 would produce a constant-airspeed trajectory that would fail to use all available airplane performance. A gain of 1 would produce a nearly constant flight-path-angle trajectory that would rapidly deplete excess airspeed. Gains of 0.3 to 0.5 effectively distribute the excess airspeed. In this effort, the gain was a function of the type of alert that triggered the recovery. The gain was set at 0.3 if a reactive alert began the recovery, and was set at 0.4 if a forward-look alert initiated the recovery. Both the positive and negative flight-path-angle target values were limited to 0.06 rad (3.4°) to prevent excessive climb or descent rates during the recovery. The commanded flight-path angle was also limited to prevent descent below the glide slope, which was assumed to be set at 0.05 rad (3°).

Flight-path-angle strategy. For this strategy, the airplane was required to fly a flight-path angle that was a function of altitude, wind-shear F-factor, and available airplane performance. If the potential inertial flight-path angle was positive, that climb gradient was maintained. If the potential inertial flight-path angle was negative, the target climb gradient was altitude dependent. Below a reference altitude H_{ref}, the strategy was to attempt to climb regardless of wind-shear strength, under the assumption that obstacles must be cleared. In the study described in reference 10, H_{ref} was 100 ft. The target flight-path angle was 0.03 rad (1.72°) at ground level and decreased linearly to level flight at H_{ref}. Above H_{ref}, the strategy maintained one-half the potential inertial flight-path angle. This feature permitted a descent to be maintained at the higher altitudes to reduce the rate at which airspeed was lost. The reference altitude was set to 100 ft for reactive-alert recoveries and 400 ft for forward-look alert recoveries. The same commanded flight-path-angle limits were applied to this strategy as were applied to the acceleration strategy.

Level strategy. The level strategy was a simplification of the flight-path-angle strategy, in that only one climb angle was targeted. Upon initiating the recovery, this strategy attempted to maintain level flight. Level flight prevents the rapid decay of airspeed associated with attempting to climb in a wind shear while taking advantage of the obstacle clearance provided above the glide slope.

Glide-slope strategy. The glide-slope strategy was meant to emulate the characteristics of the optimal-approach abort trajectories described in reference 7. That effort showed that the optimal recovery trajectory initially caused the airplane to continue to descend and later transition to a slight climb. The shallow-climb flight path was flown until the wind shear was exited. For this study, that trajectory was approximated by initially tracking the glide slope, at go-around thrust, until the altitude reached a reference altitude H_{ref}. The value of H_{ref} was 100 ft for reactive-alert recoveries and 500 ft for forward-look alert cases. After reaching H_{ref}, the strategy attempted to maintain a 0° flight-path angle until the shear was exited. The glide slope was chosen as the descent angle to provide obstacle clearance during the recovery.

Go-around strategy. The go-around strategy was flown the same as the manual strategy, except that a different initial pitch attitude was used. The intent of including the go-around strategy was to simulate the effects of reconfiguring the airplane during the recovery. This strategy was evaluated, however, both with a fixed configuration and with reconfiguration. During reconfiguration, the wing flaps were retracted to 15° and the landing gear was raised. The go-around pitch attitude was 0.17 rad (10°) for the data runs. As in the manual recovery procedure, the pitch attitude was increased if necessary to avoid a negative flight-path angle.

Results and Discussion

Energy-Height Analysis

The energy-height analysis was performed for various wind-shear strengths and alert-time values. The F-factor of the shears was varied from 0.10 to 0.30. Current-generation reactive wind-shear systems are typically set to F-factor thresholds from 0.10 to 0.15 and would probably not detect the weakest shear shown. Alert time was varied from −20 sec (reactive alert with delay) to 60 sec (forward-look alert). The results are depicted in figure 6. As previously noted, these results depict energy height rather than altitude and are independent of the recovery technique utilized. The figure shows that with a 10- to 15-sec delay in detecting the presence of the wind shear and applying go-around thrust, even a relatively weak shear results in the loss of 300 to 500 ft of energy height. An appreciation of the significance of a 300 ft loss in energy height can be gained by considering the energy height present in airplane excess airspeed. The energy-height change due to slowing from the reference approach speed (137 to 145 knots) to

the stick-shaker speed (107 knots) is approximately equivalent to a 300- or 400-ft change in altitude.

The benefit of reducing the time required to detect a wind shear can easily be seen. For each second of improvement in the time required to give a reactive alert, the energy-height loss across the event is reduced by about 40 ft. Still greater benefits are achievable with the use of forward-look wind-shear detection and alerting. Alerts given only 15 to 20 sec prior to shear entry would permit recovery from relatively strong shears with no net loss in altitude from the point where the alert was received.

Recovery-Altitude Performance

For the nonpiloted simulation data presented, the center of the microburst was located 4000 ft in horizontal distance from the initial airplane position. The geometry of the microburst encounter was varied by changing the initial altitude of the airplane. In every run, the initial trimmed airspeed of the airplane was 137 knots with the landing gear down and wing flaps set at 25°. The recovery altitude for each recovery strategy, initial altitude, alert time, and airplane configuration treatment is shown in table 2. For some of the low-altitude runs, no wind-shear alert was received, either because the aircraft contacted the ground before the delay time was achieved or because the forward-look alert time was longer than the run length. These cases are indicated by "NA." The initial altitudes varied from 100 to 900 ft above ground level in 100 ft increments, and the alert time varied from a 10-sec forward look to a 10-sec delay in 5-sec increments. The corresponding encounter altitude for each combination of initial altitude and alert time is also shown. The encounter altitude is the altitude at which the wind shear was detected and the recovery initiated. In half the runs, the airplane configuration was held constant. During the recovery in the other half of the runs, the wing flaps were retracted to the go-around position of 15°, and the landing gear was raised. Unless otherwise specified in the discussions to follow, all references to table 2 are for the fixed-configuration runs.

Of the factors explored, the factor that produced the greatest improvement in recovery altitude was the alert time. The improvement in recovery altitude with each 5-sec improvement in the alert time was generally greater than the difference in performance between recovery strategies. With initial altitudes of 500 ft or less, the effect of increasing the alert time by 5 sec was also greater than the effect of increasing the initial altitude by 100 ft. Depending on the initial altitude, the recovery-altitude increase ranged from 140 ft to 400 ft when the alert time was improved from −5 to 10 sec. Figure 7 shows aircraft trajectories from runs using the flight-path-angle strategy, from an initial altitude of 500 ft, with the alert time ranging from −10 to 10 sec. A 10-sec alert delay produced a run that came within 3 ft of the ground and involved flight at the stick-shaker angle of attack for 10 sec. An alert time of zero produced a minimum altitude of 148 ft and 11 sec of flight at the stick-shaker angle of attack. A 10-sec forward-look alert produced a run that had a minimum altitude of 404 ft and never reached the stick-shaker angle of attack. Figure 7 shows that the recovery altitude was essentially the same with alert times of 5 and 10 sec. In the 5-sec alert case, however, the minimum airspeed (not shown) was 104 knots, which is very close to the $1g$ stall speed. Any increase in the shear strength or duration would have initiated a descent. In the 10-sec alert case, the minimum airspeed was 121 knots.

The alert-time effects shown in table 2 tend to support the analytical energy-height analysis. The data for an initial altitude of 500 ft show that when a reactive alert with a 5-sec delay was given at an altitude of 315 ft, the aircraft lost an average of 291 ft of altitude. When a 10-sec forward-look alert was given at an altitude of 460 ft, the average altitude loss was only 26 ft.

Table 2 shows that no single recovery strategy, initial altitude change, or alert-time change has the best performance in all wind-shear encounter situations. For example, in the case of a 10-sec forward look and an initial altitude of 600 ft, the flight-path-angle strategy had the lowest recoveries; when the initial altitude was reduced to 200 ft, the manual strategy had the lowest recoveries. Likewise, increasing the initial altitude generally increased the recovery altitude, but not always. Improving the alert time also usually increased the recovery altitude, but had the opposite effect in certain situations. The conclusion is that no single example of improved performance can be used to select an optimum strategy or encounter scenario. Choosing a strategy for implementation would require finding a strategy that results in the best performance in the majority of the critical encounter scenarios.

Table 2 also shows that the recovery performance between strategies was generally similar. In the case of reactive alerts with initial altitudes of 500 ft or less, the difference in recovery altitudes between strategies was less than 20 ft. Above an initial altitude of 500 ft, larger differences, on the order of 50 to 90 ft, begin to appear. In each case, the strategies with the highest recovery altitudes are the ones that permit further descent during the recovery (acceleration, flight-path angle, glide slope, and pitch), while the lowest recovery altitudes were achieved with the strategies that

attempted to prevent any further descent (manual, level, and go-around).

When the strategies are compared in the runs for which a forward-look alert was given, the relative performance depended on the altitude of the encounter. With initial altitudes below 500 ft, the manual and pitch strategies had the lowest recovery altitudes. The difference in performance between the strategies lessened as the initial altitude increased, and, above an initial altitude of 600 ft, the performances of the manual and pitch strategies were essentially the same as or better than those of the other strategies. Figure 8 shows the altitude, pitch, and airspeed time histories produced by each of the strategies when the initial altitude was 300 ft and the forward-look alert time was 5 sec. The initial pitch increase and climb produced by the manual and pitch strategies (figs. 8(c) and 8(a)) caused a rapid loss of airspeed that eventually required lowering the pitch attitude to prevent a stall.

The relatively low recovery altitudes seen with the manual strategy (table 2) should not be interpreted as evidence that the technique presently being taught to air-carrier crews is not correct. First, the results show that the relative performance of this strategy is low in the case of forward-look detection, but is reasonably good in the case of reactive detection. The technique being taught to pilots is for use in situations for which a microburst has been inadvertently entered; hence, there is reactive detection. Also, the manual strategy being evaluated is only an approximation of the actual training technique. Finally, reference 3 indicates that the difference in performance between recovery strategies observed in piloted simulations may be less than the performance differences predicted in nonpiloted simulations.

Comparison of the recovery altitudes with the initial altitudes (table 2) shows that the severity of the microburst varied with altitude. In the case of a reactive alert with a 5-sec delay, for example, increasing the initial altitude from 300 ft to 400 ft increased the encounter altitude by 101 ft, but the recovery altitude decreased from an average (across the 7 strategies) of 45 ft to an average of 23 ft. Increasing the initial altitude another 100 ft, to 500 ft, increased the encounter altitude by 103 ft, but the average recovery altitude remained essentially constant at 24 ft. Above an initial altitude of 600 ft, however, the average recovery altitude increased more than 100 ft per 100 ft of increase in encounter altitude.

Figure 9 shows altitude time histories for initial altitudes of 300 ft to 700 ft with a 5-sec reactive-alert delay using the flight-path-angle strategy. The microburst effects were most severe when entered at altitudes above 110 ft and below 315 ft. Since the altitude of the maximum outflow is 120 ft, it would be expected that the wind-shear effects would be less severe below that altitude. Figure 10 shows an F-factor plot for four constant-altitude paths through the microburst; constant airspeed was assumed during the encounter. The values plotted are for altitudes of 60, 120, 240, and 480 ft. The plot shows that the largest F-factor values occur at the 120-ft altitude and that they are nearly as large as those at the 240-ft altitude. The F-factor is appreciably lower, however, at the 60-ft and 480-ft levels.

The effect of altitude on microburst severity also produced a few runs for which improving the alert time decreased the recovery altitude. Table 2 shows that, in the case of the manual strategy at an initial altitude of 300 ft, a −5-sec alert time produced a recovery altitude of 39 ft and an alert given 5 sec earlier produced a recovery altitude of 18 ft. The same phenomenon was seen with the manual strategy when changing the alert time from 0 to 5 sec at an initial altitude of 200 ft. In both scenarios, delaying the alert caused the airplane to begin the recovery while below the altitude for the maximum wind velocity; this delay reduced the severity of the wind shear. It is not suggested, however, that wind-shear detection systems be designed to intentionally delay alerts; this effect rarely occurred in the matrix, and operational factors such as boundary-layer turbulence and flight technical error may make intentional flight at such low altitudes impractical.

The effect of changing airplane configuration can be estimated from the data in table 2. In most of the reactive-alert scenarios, retracting flaps and gear resulted in a lower recovery altitude. Although the recovery altitudes were lower when the flaps were retracted to 15°, the total energy of the aircraft was higher at the minimum altitude than when the flap position remained constant. Figure 11 shows the altitude and airspeed time histories of two runs with the same initial conditions, but with one run flown with a fixed configuration and the other with flap retraction. The flight-path-angle strategy with a 5-sec delay on the alert was used. The lower altitudes seen after flap retraction appear to be the results of a temporary reduction in the flight-path angle as the flaps were retracted, even though the recovery strategy attempts to control flight-path angle. When the configuration remained fixed, the minimum energy height was about 730 ft; when the flaps were retracted, minimum energy height was about 920 ft. In the case of a reactive alert, the short-period response of retracting flaps appeared to have had a greater influence on the results than the long-period gain in energy. In the scenarios where forward-look alerting was used, changing airplane configuration had mixed effects.

In some runs, changing the configuration increased the recovery altitude, and in other runs, the opposite result occurred. For all the forward-look runs, no significant change in recovery altitude occurred when the airplane configuration was changed.

Concluding Remarks

The results of this effort show that the factor that most strongly affects a microburst recovery is the time at which the recovery is initiated. In nearly all microburst situations evaluated, initiating the recovery 5 sec earlier provided a greater recovery performance increase than could be achieved by changing the recovery strategy. Forward-look alerts given 10 sec prior to microburst entry permitted recoveries to be made with negligible altitude loss.

The results also illustrate that no single microburst scenario can be used to evaluate the relative merits of various recovery strategies. If a strategy was chosen that performed best in the majority of the microburst scenarios, a scenario could be found in which another strategy performed better. The type of alert (reactive or forward-look) used to initiate the recovery and the altitude of the microburst encounter had an effect on the type of recovery strategy that performed best. It was also possible to find a scenario in which improved wind-shear alerting decreased the recovery performance. The difficulty of recovery in a microburst model that included realistic boundary-layer and altitude effects was a function of the altitude of the microburst encounter. These factors may have serious implications in determining the most hazardous microburst encounter scenarios and in the design and certification of wind-shear systems.

Airplane configuration should not be altered toward the go-around configuration during a recovery following a reactive wind-shear alert. If the recoveries were begun just prior to entering the microburst, there appeared to be little performance effect from changing the configuration.

The baseline recovery strategy was an approximation of the manual wind-shear recovery technique that is currently being taught to air-carrier crews. This baseline strategy appeared to compare favorably with the proposed advanced recovery strategies when used in the microburst scenarios that the manual technique was designed to accommodate. These scenarios are low-altitude microburst encounters in which the hazard is not recognized until after microburst entry. Opportunity for improvement remains for scenarios in which the recovery is initiated prior to entering the microburst, that is, upon receiving a forward-look alert. Additional research is needed to validate the effects of alert-time and recovery-strategy variations in a piloted simulation environment.

NASA Langley Research Center
Hampton, VA 23665-5225
December 27, 1989

References

1. McCarthy, John; Blick, Edward F.; and Bensch, Randall R.: *Jet Transport Performance in Thunderstorm Wind Shear Conditions.* NASA CR-3207, 1979.
2. Fujita, T. Theodore: *The Downburst—Microburst and Macroburst.* SMRP-RP-210, Univ. of Chicago, 1985. (Available from NTIS as PB85 148 880.)
3. Hinton, David A.: *Piloted-Simulation Evaluation of Recovery Guidance for Microburst Wind Shear Encounters.* NASA TP-2886, DOT/FAA/DS-89/06, 1989.
4. Psiaki, Mark L.; and Stengel, Robert F.: Analysis of Aircraft Control Strategies for Microburst Encounter. AIAA-84-0238, Jan. 1984.
5. Psiaki, Mark L.; and Stengel, Robert F.: Optimal Flight Paths Through Microburst Wind Profiles. *J. Aircr.*, vol. 23, no. 8, Aug. 1986, pp. 629–635.
6. Miele, A.; Wang, T.; and Melvin, W. W.: *Optimal Flight Trajectories in the Presence of Windshear. Part 4, Numerical Results, Take-Off.* Aero-Astronaut. Rep. No. 194, Rice Univ., 1985.
7. Miele, A.; Wang, T.; Tzeng, C. Y.; and Melvin, W. W.: *Optimal Abort Landing Trajectories in the Presence of Windshear.* Aero-Astronaut. Rep. No. 215, Rice Univ., 1987.
8. Miele, A.; Wang, T.; and Melvin, W. W.: *Maximum Survival Capability of an Aircraft in a Severe Windshear.* Aero-Astronaut. Rep. No. 213, Rice Univ., 1986.
9. Miele, A.; Wang, T.; and Melvin, W. W.: *Gamma Guidance Schemes and Piloting Implications for Flight in a Windshear.* Aero-Astronaut. Rep. No. 212, Rice Univ., 1986.
10. Hinton, David A.: *Flight-Management Strategies for Escape From Microburst Encounters.* NASA TM-4057, 1988.
11. Boeing Co.: *Wind Shear Training Aid. Volume 1—Overview Pilot Guide, Training Program.* Contract DFTAO-1-86-C-00005, Feb. 1987. (Available from NTIS as PB88 127 196.)
12. Oseguera, Rosa M.; and Bowles, Roland L.: *A Simple, Analytic 3-Dimensional Downburst Model Based on Boundary Layer Stagnation Flow.* NASA TM-100632, 1988.
13. Proctor, F. H.: *The Terminal Area Simulation System—Volume I: Theoretical Formulation.* NASA CR-4046, DOT/FAA/PM-86/50, I, 1987.
14. Proctor, F. H.: *The Terminal Area Simulation System—Volume II: Verification Cases.* NASA CR-4047, DOT/FAA/PM-86/50, II, 1987.

Table 1. Strategies Evaluated and Gains Used

Strategy	Gain or parameter	Value used
Manual	Initial pitch target	0.261 rad (15°)
Pitch	Pitch target	0.23 rad (13°)
Acceleration	λ	0.3 for reactive alert 0.4 for forward alert
Flight-path angle	H_{ref}	100 ft for reactive alert 400 ft for forward alert
Level	None	
Glide slope	H_{ref}	100 ft for reactive alert 500 ft for forward alert
Go-around	Initial pitch target	0.175 rad (10°)

Table 2. Recovery Altitude for Each Run

[Numbers in parentheses indicate altitude (in ft) at which wind shear was detected for a particular initial altitude and alert time; numbers to left of slants are recovery altitudes with a fixed airplane configuration; numbers to right of slants are recovery altitudes with variable airplane configuration.]

Initial altitude, ft	Strategy	Recovery altitude, ft, for alert time, sec, of—				
		−10	−5	0	5	10
100	Manual	NA	NA	(38) 30/	(88) 71/	NA
	Pitch	NA	NA	30/28	71/68	NA
	Acceleration	NA	NA	0/0	71/68	NA
	Flight path	NA	NA	30/28	71/68	NA
	Level	NA	NA	30/28	71/68	NA
	Glide slope	NA	NA	30/28	71/68	NA
	Go-around	NA	NA	30/28	71/68	NA
200	Manual	NA	(26) 12/	(74) 30/	(119) 15/	(164) 89/
	Pitch	NA	12/10	50/62	65/108	155/154
	Acceleration	NA	8/5	57/56	105/104	151/150
	Flight path	NA	12/10	64/62	109/108	155/154
	Level	NA	12/10	64/62	109/108	155/154
	Glide slope	NA	12/10	64/62	109/108	155/154
	Go-around	NA	12/10	64/62	109/108	155/154
300	Manual	(59) 21/	(111) 39/	(159) 18/	(203) 22/	(250) 153/
	Pitch	21/12	45/31	37/50	74/120	221/238
	Acceleration	21/12	54/36	67/52	101/138	237/235
	Flight path	21/12	40/28	81/55	120/191	239/238
	Level	21/12	41/28	42/49	156/189	239/238
	Glide slope	21/12	53/35	84/83	134/192	239/238
	Go-around	21/12	41/28	42/50	141/189	239/238
400	Manual	(161) 12/	(212) 13/	(261) 20/	(306) 88/	(354) 312/
	Pitch	12/0	29/12	55/43	158/186	303/320
	Acceleration	12/0	31/11	74/45	163/212	338/336
	Flight path	12/0	31/11	85/57	198/279	344/342
	Level	12/0	13/3	28/39	225/282	344/342
	Glide slope	12/0	31/11	75/61	187/276	344/342
	Go-around	12/0	14/3	29/40	222/282	344/342
500	Manual	(264) 3/	(315) 11/	(363) 45/	(411) 226/	(460) 450/
	Pitch	3/0	43/17	123/96	252/259	395/407
	Acceleration	3/0	30/4	129/77	268/328	442/441
	Flight path	3/0	30/4	148/99	329/392	404/406
	Level	3/0	11/0	48/74	330/392	450/448
	Glide slope	3/0	30/4	146/107	286/389	450/448
	Go-around	3/0	11/0	49/75	330/391	450/448

Table 2. Concluded

Initial altitude, ft	Strategy	Recovery altitude, ft, for alert time, sec, of—				
		−10	−5	0	5	10
600		(366)	(416)	(466)	(515)	(566)
	Manual	41/	57/	154/	388/	555/
	Pitch	39/1	129/72	238/208	345/344	494/503
	Acceleration	41/3	108/48	261/207	410/474	552/551
	Flight path	41/3	108/48	271/234	403/404	474/505
	Level	41/3	57/28	156/205	467/500	555/554
	Glide slope	41/3	108/48	240/239	468/486	487/486
	Go-around	41/3	57/29	155/206	467/499	555/554
700		(466)	(516)	(568)	(619)	(672)
	Manual	149/	160/	288/	553/	655/
	Pitch	141/69	252/193	326/294	435/402	592/597
	Acceleration	149/75	241/168	393/347	541/599	655/653
	Flight path	149/75	241/168	395/366	469/491	580/614
	Level	149/75	160/127	286/344	596/599	655/653
	Glide slope	149/75	241/168	339/339	483/483	483/482
	Go-around	149/75	160/126	288/346	596/598	655/653
800		(567)	(617)	(699)	(721)	(776)
	Manual	284/	289/	418/	696/	756/
	Pitch	272/198	353/316	414/380	527/491	690/692
	Acceleration	283/208	374/309	518/480	678/700	755/752
	Flight path	283/208	374/309	507/491	578/601	687/725
	Level	284/208	288/257	416/479	705/702	756/752
	Glide slope	283/208	374/309	439/439	485/484	484/483
	Go-around	284/208	289/257	418/482	704/701	756/752
900		(667)	(717)	(771)	(824)	(880)
	Manual	409/	409/	536/	810/	863/
	Pitch	394/328	444/411	502/465	617/579	786/788
	Acceleration	409/341	498/440	636/604	795/803	860/859
	Flight path	409/341	498/440	613/607	686/714	804/848
	Level	409/341	408/378	534/601	808/806	863/860
	Glide slope	409/341	498/440	538/538	538/539	538/540
	Go-around	409/341	409/378	536/603	807/805	863/860
Average of all heights	Manual	131	124	171	319	479
	Pitch	126/87	163/133	197/181	283/284	455/462
	Acceleration	131/91	168/128	237/208	348/381	499/497
	Flight path	131/91	167/127	244/222	329/361	461/479
	Level	131/91	124/104	178/209	385/405	502/500
	Glide slope	131/91	168/128	217/211	307/336	398/397
	Go-around	131/91	124/104	179/210	383/405	502/500
Average all runs		130/91	148/121	203/207	336/362	471/473

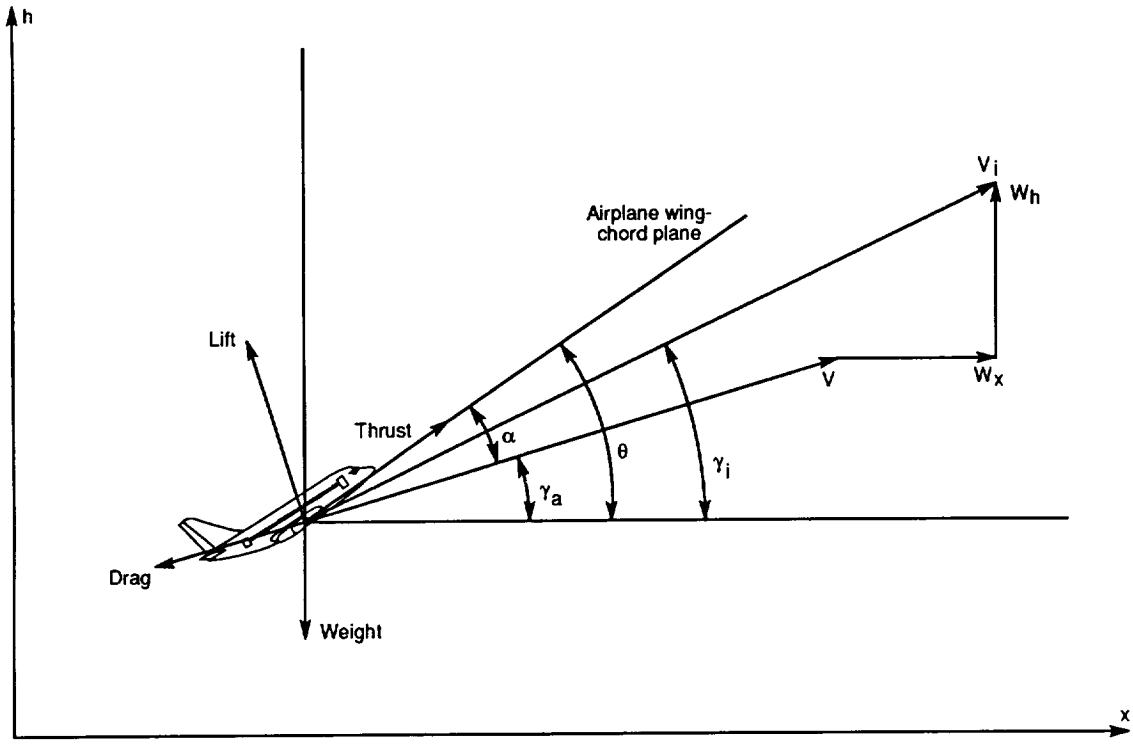

Figure 1. Flight path and wind coordinate system.

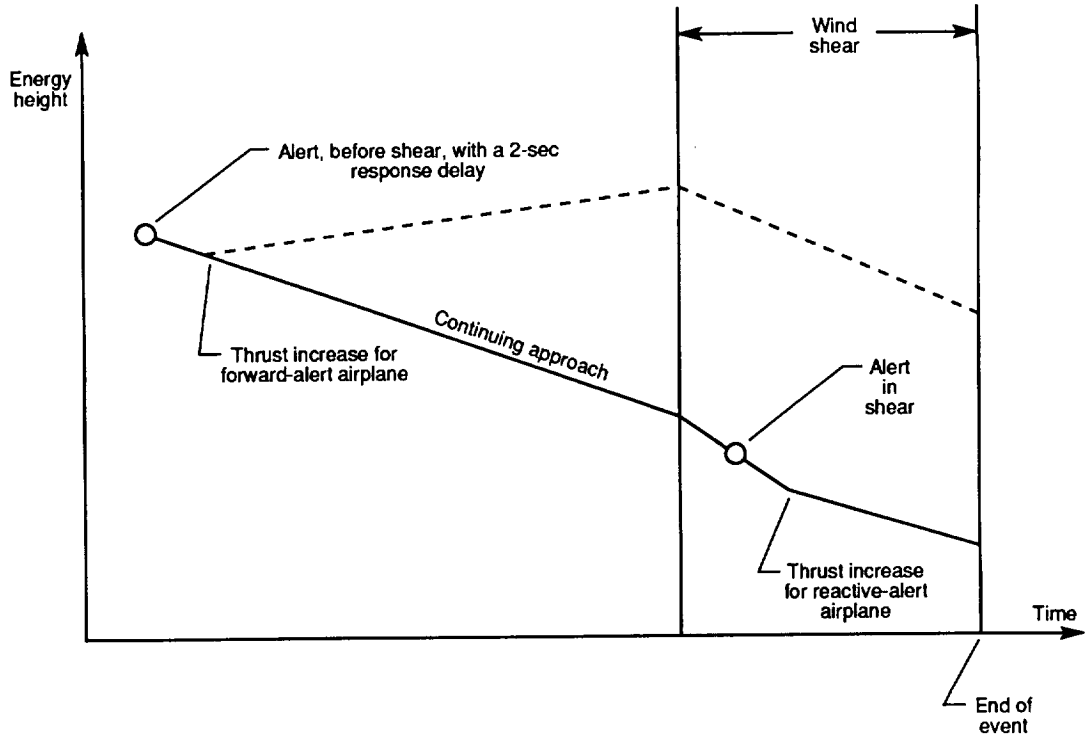

Figure 2. Scenario for energy-height analysis.

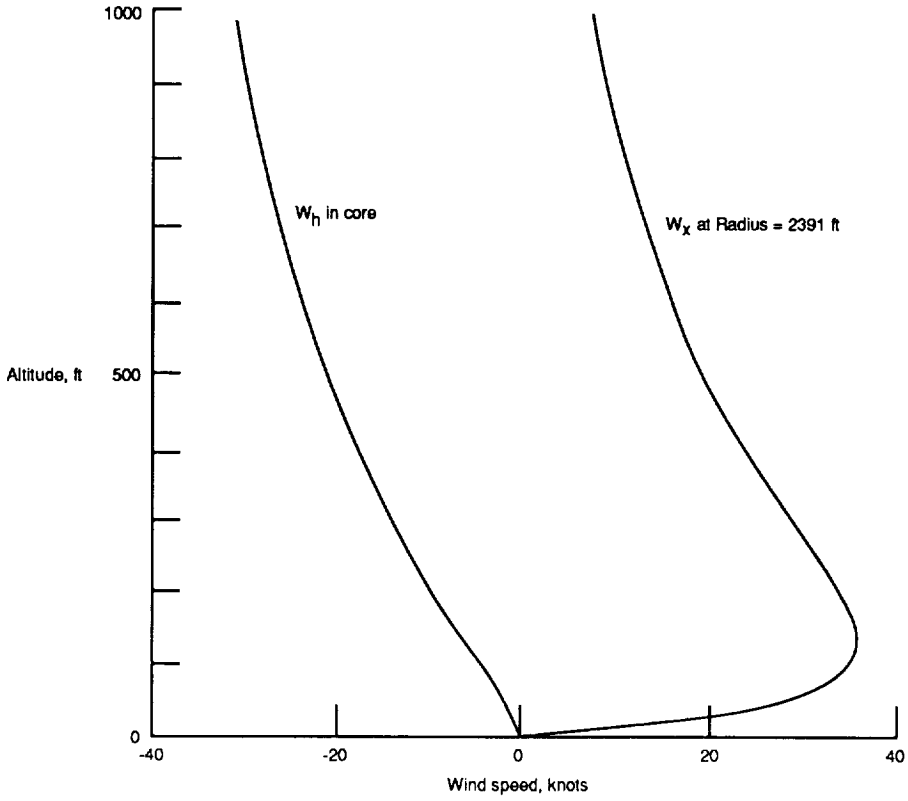

Figure 3. Microburst model altitude profiles.

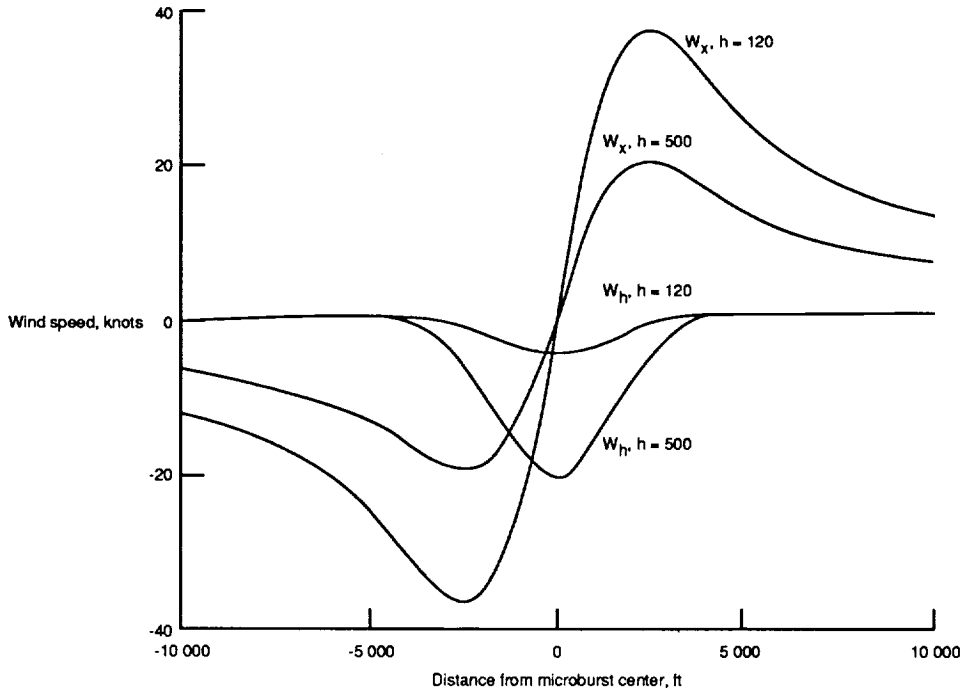

Figure 4. Microburst model radial and vertical wind components.

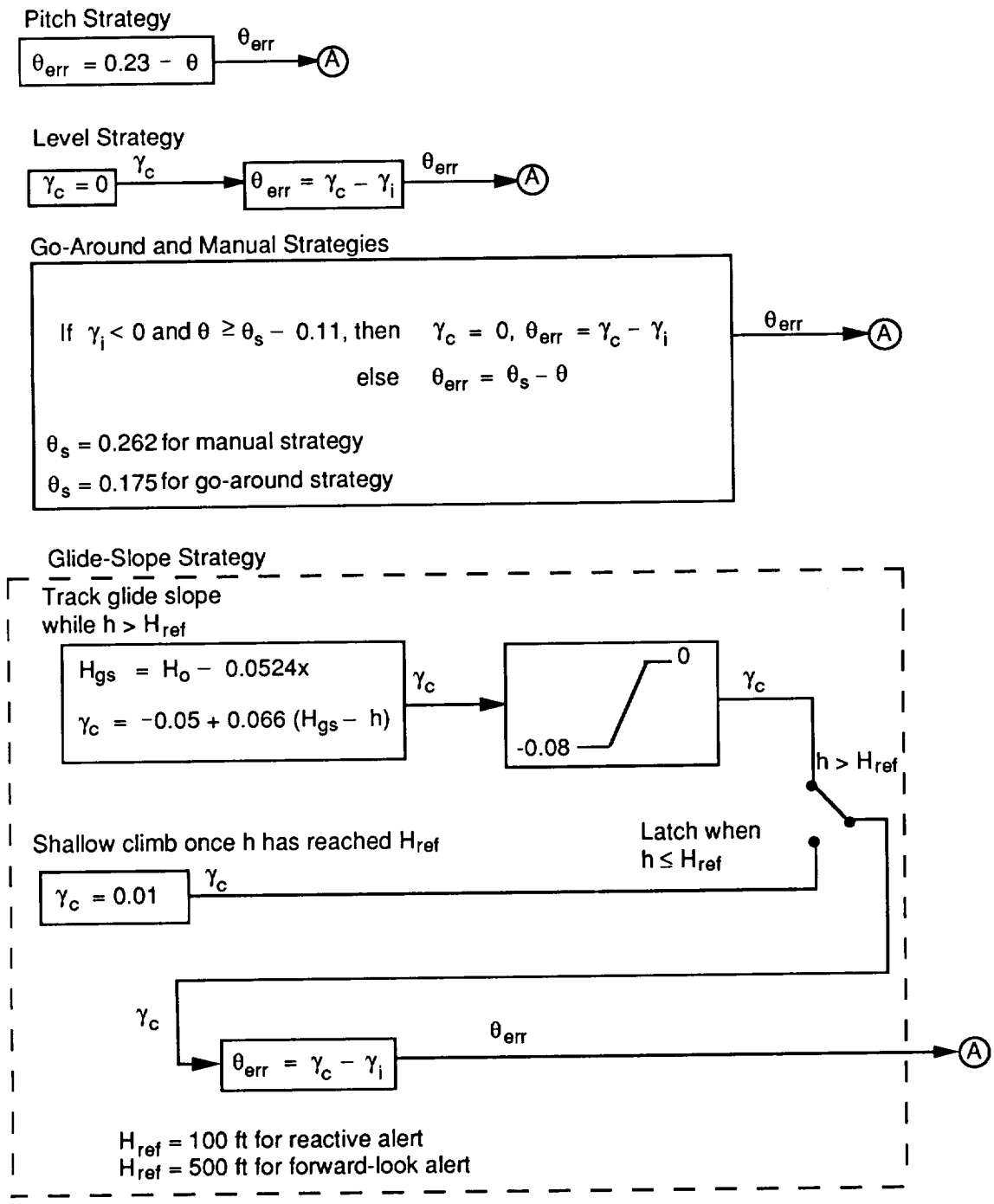

Figure 5. Recovery-strategy control laws. All angles expressed in radians.

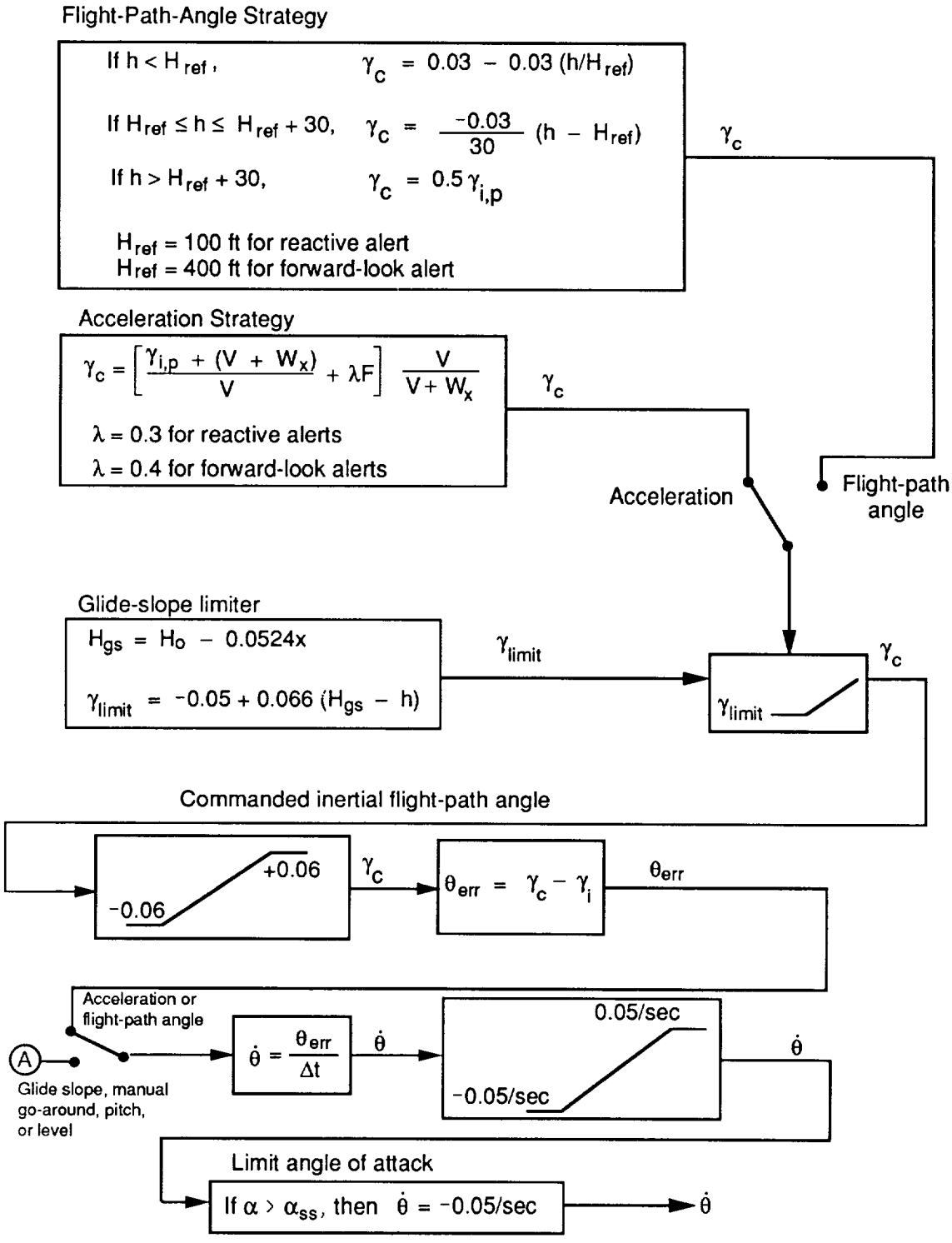

Figure 5. Concluded.

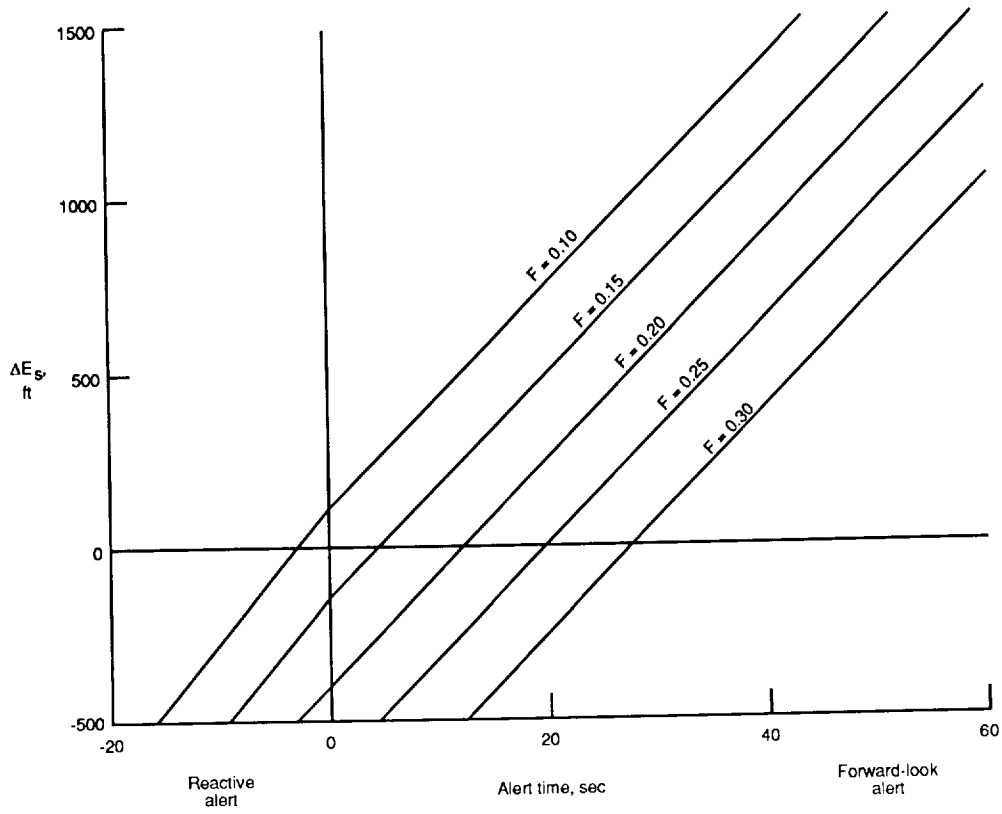

Figure 6. Change in energy height across an event.

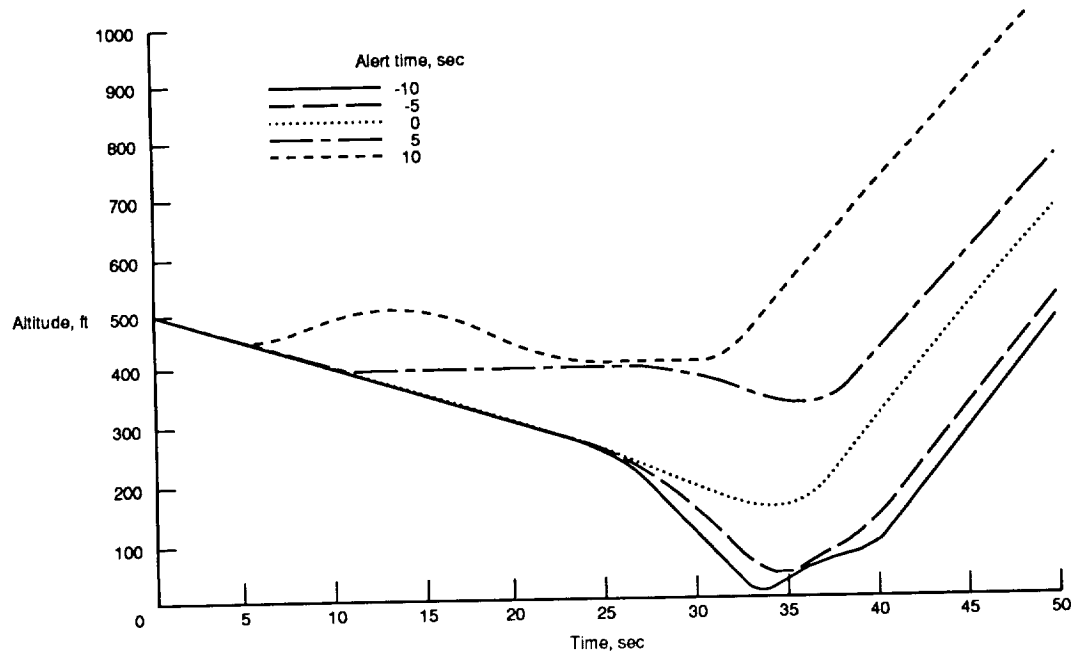

Figure 7. Effect of varying the wind-shear alert time.

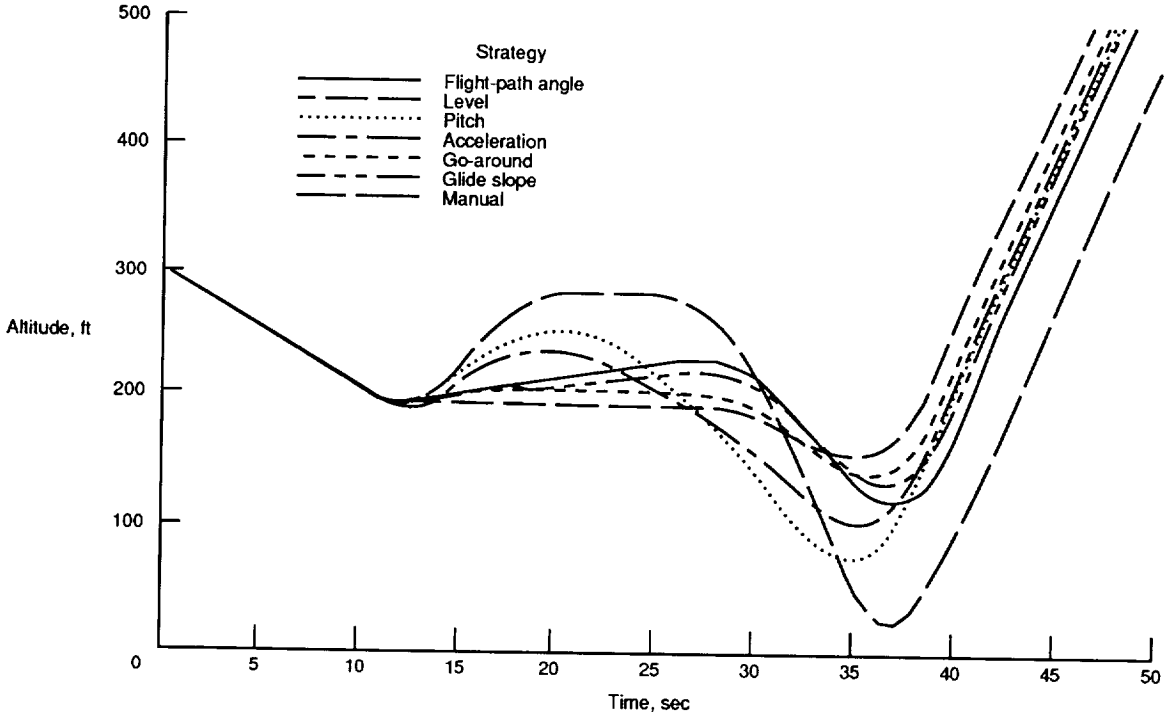

(a) Altitude.

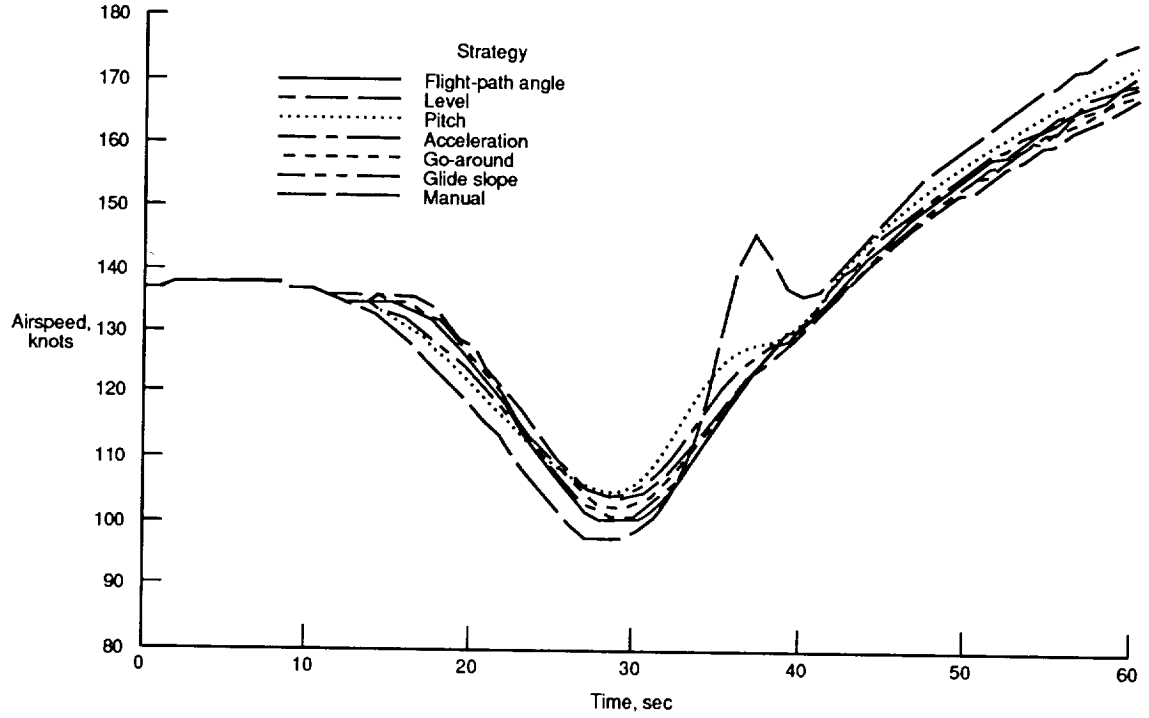

(b) Airspeed.

Figure 8. Time-history results of all tested strategies. Forward-look alert time is 5 sec.

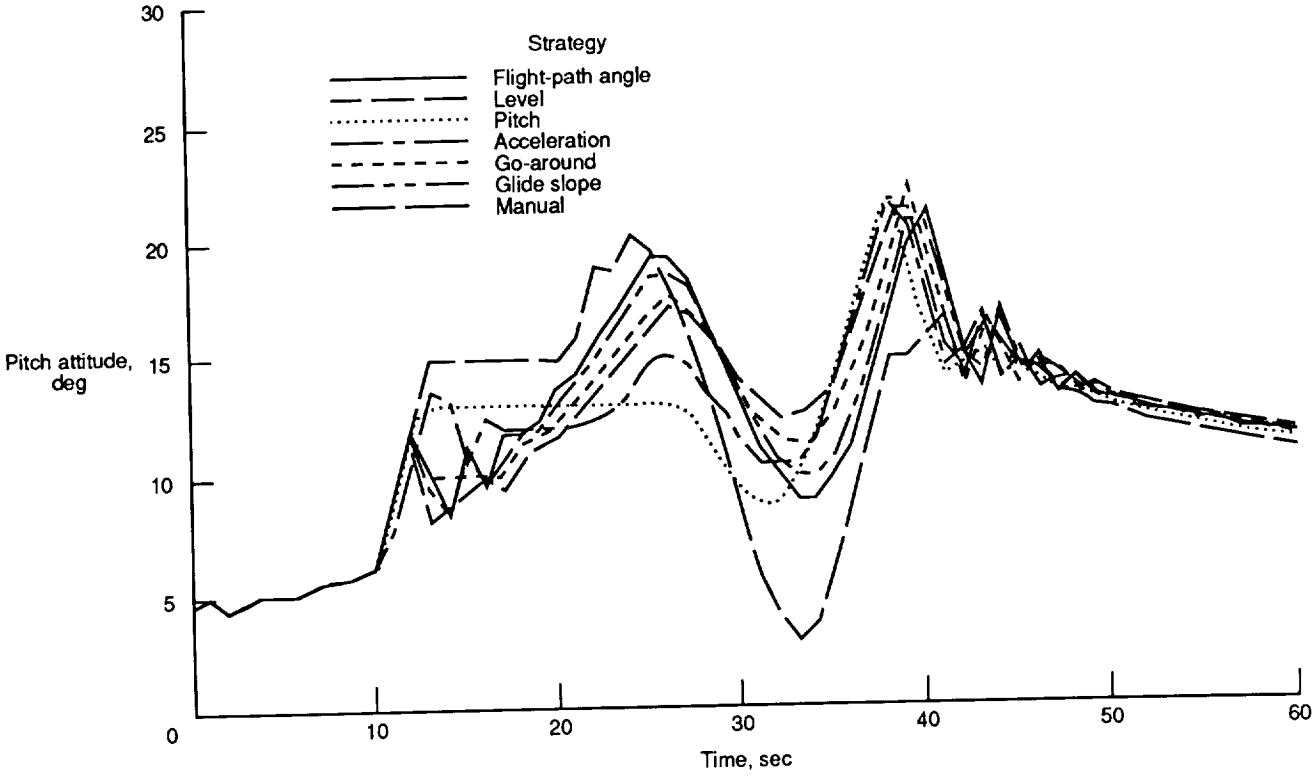

(c) Pitch.

Figure 8. Concluded.

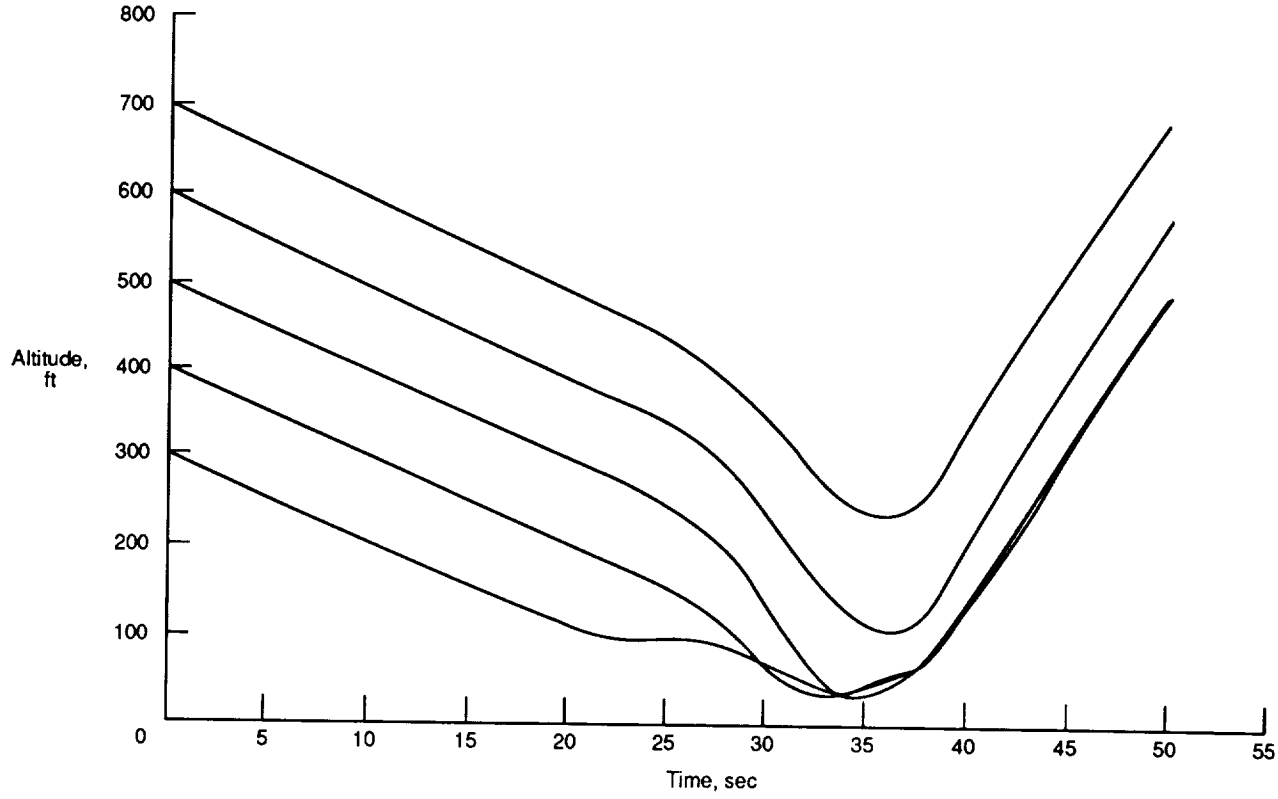

Figure 9. Effect of varying altitude of microburst encounter. Flight-path-angle strategy with a 5-sec reactive-alert delay.

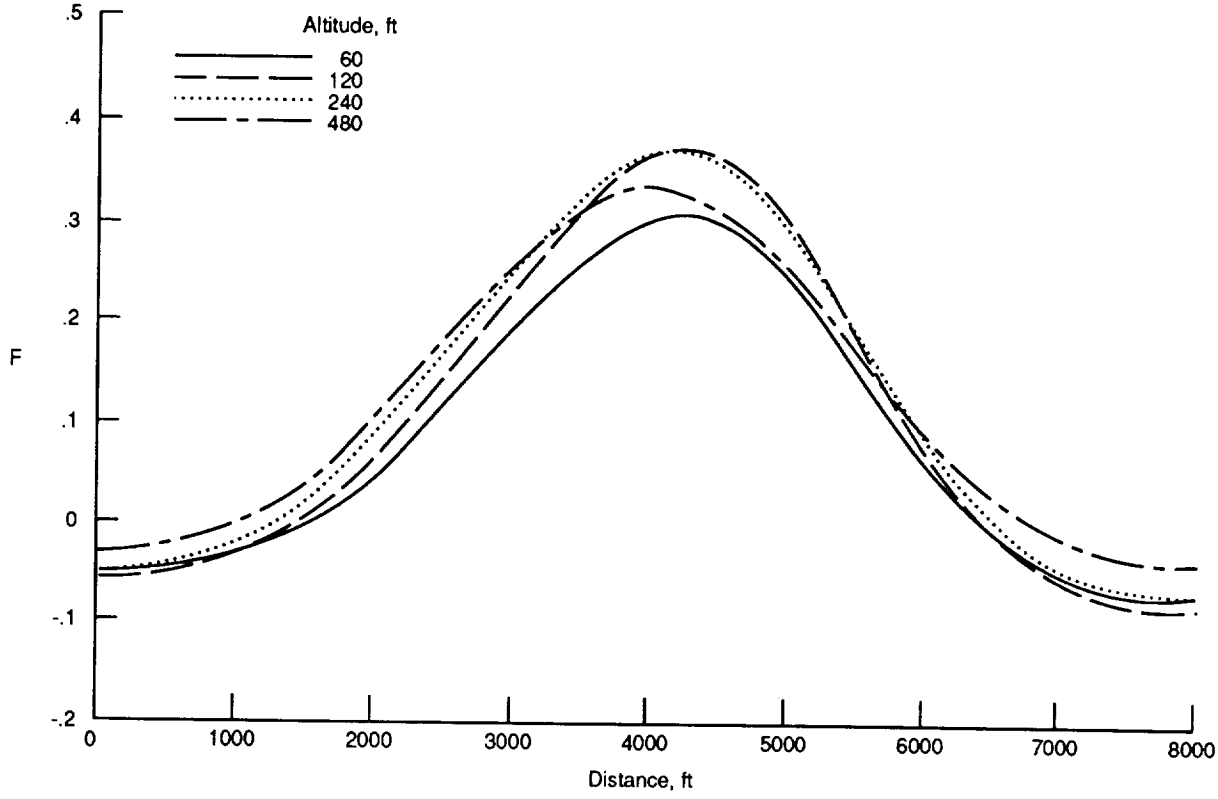

Figure 10. F-factor in four constant-altitude, constant-airspeed paths through microburst model.

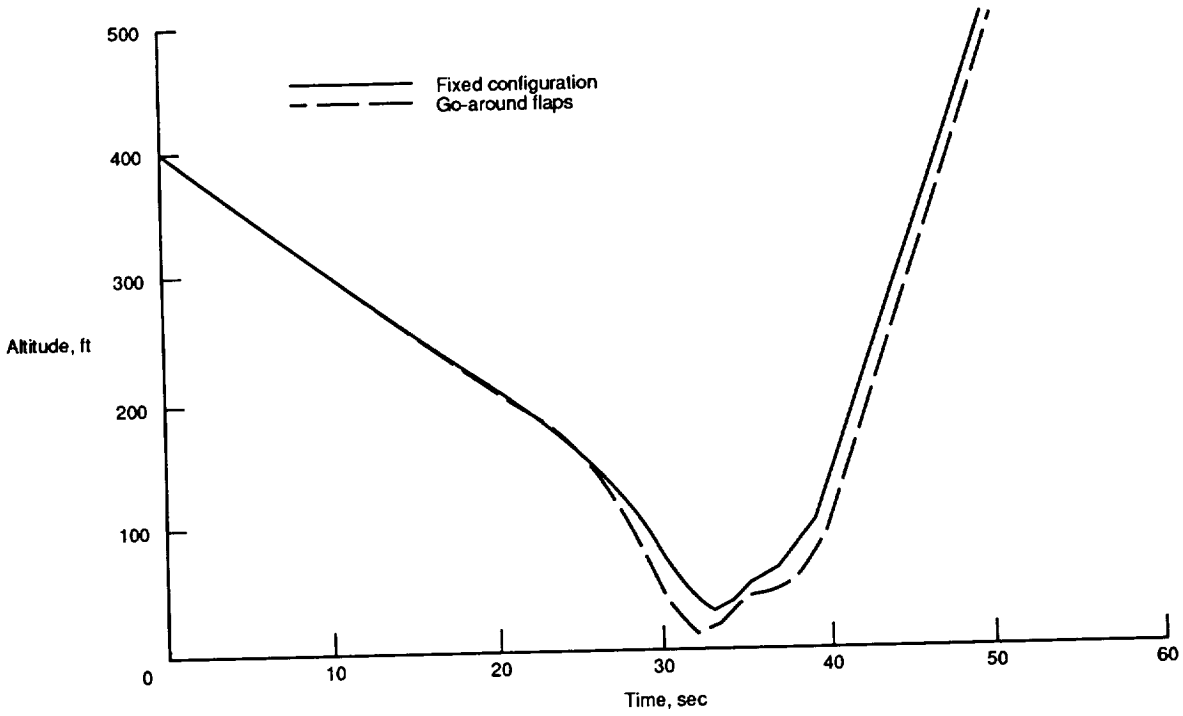

(a) Altitude.

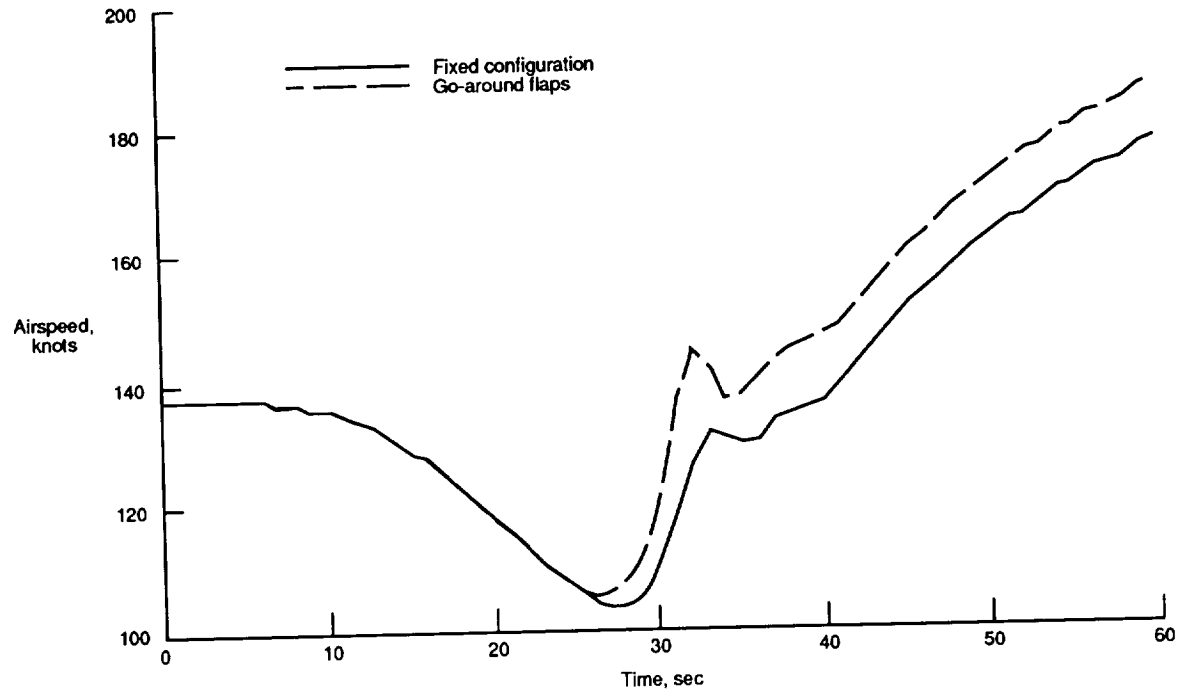

(b) Airspeed.

Figure 11. Effect of changing airplane configuration during recovery. Flight-path-angle strategy with a 5-sec reactive-alert delay.

NASA
National Aeronautics and Space Administration

Report Documentation Page

1. Report No.	2. Government Accession No.	3. Recipient's Catalog No.
NASA TM-4158 DOT/FAA/DS-89/35		

4. Title and Subtitle	5. Report Date
Relative Merits of Reactive and Forward-Look Detection for Wind-Shear Encounters During Landing Approach for Various Microburst Escape Strategies	February 1990
	6. Performing Organization Code
7. Author(s) David A. Hinton	8. Performing Organization Report No. L-16622
9. Performing Organization Name and Address NASA Langley Research Center Hampton, VA 23665-5225	10. Work Unit No. 505-66-41-41
	11. Contract or Grant No.
12. Sponsoring Agency Name and Address National Aeronautics and Space Administration Washington, DC 20546-0001 and Department of Transportation, Washington, D.C. 20590	13. Type of Report and Period Covered Technical Memorandum
	14. Sponsoring Agency Code

15. Supplementary Notes
Joint NASA and FAA report.

16. Abstract

This paper describes an effort to quantify the benefits of airborne forward-look wind-shear detection and to develop and test a candidate set of strategies for recovery from inadvertent microburst encounters during the landing approach, given the utilization of both reactive-only and forward-look wind-shear detection. Candidate strategies were developed and evaluated using a nonpiloted simulation consisting of a point-mass model of a transport-category airplane flying through an analytical microburst model. The results indicate that the factor that most strongly affects a microburst recovery is the time at which the recovery is initiated. Forward-look alerts given 10 sec prior to microburst entry permitted recoveries to be made with negligible altitude loss. The results also show that no single recovery strategy performed best in every microburst scenario tested. An approximation of the manual wind-shear recovery technique that is currently being taught to air-carrier crews was used as a baseline recovery strategy. This strategy compared favorably with the proposed advanced recovery strategies in the microburst scenarios that the manual technique was designed to accommodate.

17. Key Words (Suggested by Authors(s))	18. Distribution Statement
Wind shear Guidance Crew alerting Remote sensing Microburst Flight safety Forward-look detection	Unclassified—Unlimited Subject Category 08

19. Security Classif. (of this report)	20. Security Classif. (of this page)	21. No. of Pages	22. Price
Unclassified	Unclassified	22	A03

NASA FORM 1626 OCT 86

For sale by the National Technical Information Service, Springfield, Virginia 22161-2171

NASA-Langley, 1990